# Performance Analysis of Single Carrier Coherent and Noncoherent Modulation under I/Q Imbalance

Bassant Selim*, Sami Muhaidat*, Paschalis C. Sofotasios*,‡, Bayan S. Sharif*, Thanos Stouraitis*, George K. Karagiannidis§, and Naofal Al-Dhahir¶

*Department of Electrical and Computer Engineering, Khalifa University of Science and Technology, 127788, Abu Dhabi, United Arab Emirates
e-mail: {bassant.selim; sami.muhaidat; paschalis.sofotasios; bayan.sharif; thanos.stouraitis}@kustar.ac.ae
‡Department of Electronics and Communications Engineering, Tampere University of Technology, FI-33101, Tampere, Finland, (e-mail: paschalis.sofotasios@tut.fi)
§Department of Electrical and Computer Engineering, Aristotle University of Thessaloniki, GR-51124, Thessaloniki, Greece, (e-mail: geokarag@auth.gr)
¶Department of Electrical and Computer Engineering, University of Texas at Dallas, TX 75080, Dallas, USA, (e-mail: aldhahir@utdallas.edu)

***Abstract*—In-phase/quadrature-phase Imbalance (IQI) is considered a major performance-limiting impairment in direct-conversion transceivers. Its effects become even more pronounced at higher carrier frequencies such as the millimeter-wave frequency bands considered for 5G systems. In this work, we quantify the effects of IQI on the performance of different modulations under multipath fading channels. This is realized by developing a comprehensive framework for the symbol error rate (SER) analysis of coherent phase shift keying (PSK), noncoherent differential phase shift keying (DPSK) and noncoherent frequency shift keying (FSK) under IQI effects. In this context, the moment generating function of the signal-to-interference-plus-noise-ratio is first derived for single-carrier systems suffering from transmitter (TX) IQI only, receiver (RX) IQI only and joint TX/RX IQI. Capitalizing on this, we derive analytic expressions for the SER of the different modulation schemes considered. These expressions are corroborated with simulation results and they provide insights into the dependence of IQI on the system parameters. We further demonstrate that, while in some cases, IQI can cause a slight degradation of the SER performance and, hence, it can be neglected, in other cases it should be compensated in order to achieve a reliable communication link.**

## I. Introduction

The emergence of the Internet of Things (IoT) along with the ever-increasing demands of the mobile Internet impose high spectral efficiency, low latency and massive connectivity requirements on fifth generation (5G) wireless networks and beyond. Accordingly, next-generation wireless communication systems are anticipated to support heterogeneous devices for various standards and services with particularly high throughput and low latency requirements. This applies to both large scale and small scale network set ups, which calls for flexible and software reconfigurable transceivers that are capable of supporting the desired quality of service expectations. To this end, direct conversion transceivers, which employ quadrature up/down conversion to convert the radio-frequency (RF) signal, have attracted considerable attention owing to their suitability for higher levels of integration and their reduced cost and power consumption, since they require neither external intermediate frequency filters nor image rejection filters.

However, in practical communication scenarios, direct-conversion transceiver architectures inevitably suffer from RF front-end related impairments, including in-phase/quadrature-phase imbalances (IQI), which ultimately limit the overall system performance. In this context, IQI, which refers to the amplitude and phase mismatch between the I and Q branches of a transceiver, leads to imperfect image rejection resulting to performance degradation of both conventional and emerging communication systems [1]–[3] and the references therein. In ideal scenarios, the I and Q branches of a mixer have equal amplitude and a phase shift of $90^{\circ}$, providing an infinite attenuation of the image band; however, in practice, direct-conversion transceivers are sensitive to certain analog front-end related impairments that introduce errors in the phase shift as well as mismatches between the amplitudes of the I and Q branches, which corrupt the down-converted signal constellation, thereby increasing the overall error rate [1].

It is recalled that depending on the receiver's (RX) ability to exploit knowledge of the carrier's phase to detect the signals, the detection can be classified into coherent and noncoherent [2]. It is well known that coherent information detection requires full knowledge of the channel state information (CSI) at the receiver. On the other hand, noncoherent detection has been proposed as an efficient technique particularly for low-power wireless systems such as wireless sensor networks and relay networks [4]. It has been further demonstrated that, in the context of massive multi-input multi-output (MIMO) systems, the pilot overhead could exhaust needed resources and, hence, noncoherent systems could lead to a better spectral efficiency [5]. Another main advantage of these schemes stems from the fact that they simplify the detection, since they eliminate the need for channel estimation and tracking, which

978-1-5386-6355-4/18/$31.00 

reduces the cost and complexity of the receiver [6], [7]. However, this comes at the cost of higher error rate or lower spectral efficiency; as a result, selecting the most suitable modulation scheme depends on the considered application and both noncoherent and coherent detection are efficiently implemented, accordingly, in practical systems.

Furthermore, it is noted that RF front-end impairments constitute a core issue in the performance of conventional and emerging receivers as they affect considerably the performance of wireless communication systems. Nevertheless, these detrimental effects are typically neglected in the majority of analysis of such systems. To our best knowledge, the effects of RF impairments in noncoherent systems have been overlooked in the open literature so far, apart from some sporadic results [8]–[12]. In addition, the existing results on coherent detection are largely limited to particular scenarios, and do not provide a comprehensive treatment of IQI. Motivated by this, the present work is devoted to the quantification and analysis of these effects in wireless communications over multipath fading channels. To this end, the main objective is to develop a general framework for the comprehensive analysis of coherent and noncoherent modulation schemes under different IQI scenarios. In this context, we consider single-carrier systems and we quantify the effects of transmitter (TX) IQI, RX IQI and joint TX/RX IQI for $M$-ary phase shift keying ($M$-PSK), $M$-ary differential phase shift keying ($M$-DPSK) and $M$-ary frequency shift keying ($M$-FSK) constellations over Rayleigh fading channels.

*Notations*

Unless otherwise stated, $(\cdot)^*$ denotes conjugation and $j = \sqrt{-1}$. The operators $\mathbb{E}[\cdot]$ and $|\cdot|$ denote statistical expectation and absolute value operations, respectively. Also, $f_X(x)$ and $F_X(x)$ denote the probability distribution function (PDF) and cumulative distribution function (CDF) of $X$, respectively while $\mathcal{M}_X(s)$ represents the moment-generating function (MGF) associated with $X$. Finally, the subscripts $t/r$ denote the up/down-conversion process at the TX/RX, respectively.

## II. System and Signal Model

We assume that a signal, $s$, is transmitted over a flat fading wireless channel, $h$, which follows a Rayleigh distribution and is subject to additive white Gaussian noise, $n$. Assuming also that the TX/RX are equipped with a single antenna, we first revisit the signal model for the considered *M*-ary PSK, DPSK and FSK modulation schemes. At the receiver RF front end, the received RF signal undergoes various processing stages including filtering, amplification, and analog I/Q demodulation (down-conversion) to baseband and sampling. Assuming an ideal RF front end, the baseband equivalent received signal is represented as $r_{\text{id}} = hs + n$, where $h$ denotes the channel coefficient and $n$ is the circularly symmetric complex additive white Gaussian noise (AWGN) signal. The instantaneous signal to noise ratio (SNR) per symbol at the receiver input is given by $\gamma_{\text{id}} = E_s |h|^2 / N_0$, where $E_s$ is the energy per transmitted symbol and $N_0$ denotes the single-sided AWGN power spectral density. It is assumed that the RF carriers are up/down converted to the baseband by direct conversion architectures. Also, we assume frequency independent IQI caused by the gain and phase mismatches of the I and Q mixers. In this context, the time-domain baseband representation of the IQI impaired signal is given by $g_{\text{IQI}} = \mu_{t/r} g_{\text{id}} + \nu_{t/r} g_{\text{id}}^*$ [13], where $g_{\text{id}}$ is the baseband IQI-free signal and $g_{\text{id}}^*$ is due to IQI. Furthermore, the IQI coefficients $\mu_{t/r}$ and $\nu_{t/r}$ are given by

$$\begin{Bmatrix} \mu_t \\ \nu_t \end{Bmatrix} = \frac{1\{\pm\}\epsilon_t e^{\{\pm\} j\phi_t}}{2} \tag{1}$$

and

$$\begin{Bmatrix} \mu_r \\ \nu_r \end{Bmatrix} = \frac{1\{\pm\}\epsilon_r e^{\{\mp\} j\phi_r}}{2} \tag{2}$$

where $\epsilon_{t/r}$ and $\phi_{t/r}$ denote the TX/RX amplitude and phase mismatch levels, respectively. It is noted that for ideal RF front-ends, $\phi_{t/r} = 0^\circ$ and $\epsilon_{t/r} = 1$, which implies that $\mu_{t/r} = 1$ and $\nu_{t/r} = 0$. Moreover, the TX/RX image rejection ratio (IRR) is given by $\text{IRR}_{t/r} = |\mu_{t/r}|^2 / |\nu_{t/r}|^2$.

In what follows, we derive novel analytic expressions for the signal-to-interference-plus-noise-ratio (SINR) PDF, CDF and MGF of single-carrier systems in the presence of IQI.

### A. TX IQI and ideal RX:

This case assumes that the RX RF front-end is ideal, while the TX experiences IQI. Based on this, the baseband equivalent transmitted signal is expressed as $s_{\text{IQI}} = \mu_t s + \nu_t s^*$, while the baseband equivalent received signal is given by $h s_{\text{IQI}} + n = \mu_t hs + \nu_t hs^* + n$. Hence, the instantaneous SINR per symbol at the input of the receiver is given by

$$\gamma_{\text{IQI}} = \frac{|\mu_t|^2}{|\nu_t|^2 + \frac{1}{\gamma_{\text{id}}}}. \tag{3}$$

### B. RX IQI and ideal TX:

This case assumes that the TX RF front-end is ideal, while the RX is subject to IQI. Hence, the baseband equivalent received signal is given by $r_{\text{IQI}} = \mu_r hs + \nu_r h^* s^* + \mu_r n + \nu_r n^*$. Therefore, the instantaneous SINR per symbol at the RX input is expressed as

$$\gamma_{\text{IQI}} = \frac{|\mu_r|^2}{|\nu_r|^2 + \frac{|\mu_r|^2 + |\nu_r|^2}{\gamma_{\text{id}}}}. \tag{4}$$

### C. Joint TX/RX IQI:

This case assumes that both TX and RX are impaired by IQI and the baseband equivalent received signal is given by

$$r_{\text{IQI}} = (\xi_{11} h + \xi_{22} h^*) s + (\xi_{12} h + \xi_{21} h^*) s^* + \mu_r n + \nu_r n^* \tag{5}$$

where $\xi_{11} = \mu_r \mu_t$, $\xi_{22} = \nu_r \nu_t^*$, $\xi_{12} = \mu_r \nu_t$, and $\xi_{21} = \nu_r \mu_t^*$. Based on this, the instantaneous SINR per symbol at the RX input is given by

$$\gamma_{\text{IQI}} = \frac{E_s |\xi_{11} h + \xi_{22} h^*|^2}{E_s |\xi_{12} h + \xi_{21} h^*|^2 + \left(|\mu_r|^2 + |\nu_r|^2\right) N_0}. \tag{6}$$

Given that for direct conversion transceivers, the IRR is typically in the range of $20-40$dB [14], it can be safely assumed that $|\xi_{11}h|^2+|\xi_{22}h^*|^2 \gg 2\Re\left[\xi_{11}h\xi_{22}^*h\right]$ and $|\xi_{12}h|^2+|\xi_{21}h^*|^2 \gg 2\Re\left[\xi_{12}h\xi_{21}^*h\right]$. Hence, it follows that the SINR can be approximated as

$$\gamma_{\text{IQI}} \approx \frac{|\xi_{11}|^2+|\xi_{22}|^2}{|\xi_{12}|^2+|\xi_{21}|^2+\frac{|\mu_r|^2+|\nu_r|^2}{\gamma_{\text{id}}}}. \tag{7}$$

## III. MGF of the Received SINR with IQI

The MGF is an important statistical metric and constitutes a convenient tool in digital communication systems over fading channels [15]. In what follows, we derive a generalized closed form expression for the SINR MGF of single-carrier systems in the presence of IQI, which will be particularly useful in the subsequent error rate analysis.

With the aid of (3), (4) and (7), the I/Q impaired SINR can be expressed as

$$\gamma_{\text{IQI}} = \frac{\alpha}{\beta+\frac{A}{\gamma_{\text{id}}}} \tag{8}$$

where $\alpha$, $\beta$, and $A$ are given in Table I.

TABLE I: IQI parameters

| | $\alpha$ | $\beta$ | $A$ |
|---|---|---|---|
| TX IQI | $\lvert\mu_t\rvert^2$ | $\lvert\nu_t\rvert^2$ | 1 |
| RX IQI | $\lvert\mu_r\rvert^2$ | $\lvert\nu_r\rvert^2$ | $\lvert\mu_r\rvert^2+\lvert\nu_r\rvert^2$ |
| Joint TX/RX IQI | $\lvert\xi_{11}\rvert^2+\lvert\xi_{22}\rvert^2$ | $\lvert\xi_{12}\rvert^2+\lvert\xi_{21}\rvert^2$ | $\lvert\mu_r\rvert^2+\lvert\nu_r\rvert^2$ |

Hence, the CDF of $\gamma_{\text{IQI}}$ is obtained as

$$F_{\gamma_{IQI}}(x) = F_{\gamma_{id}}\left(\frac{A}{\frac{\alpha}{x}-\beta}\right) \tag{9}$$

where $\gamma_{id}$ is the IQI free SNR, which follows an exponential distribution. Hence, assuming TX and/or RX IQI, the corresponding SINR CDF is given by

$$F_{\gamma_{\text{IQI}}}(x) = 1-e^{-\frac{A}{\overline{\gamma}\left(\frac{\alpha}{x}-\beta\right)}}, \qquad 0 \le x \le \frac{\alpha}{\beta} \tag{10}$$

where $\overline{\gamma} = E_s/N_0$ denotes the average SNR. Given that $f_{\gamma_{\text{IQI}}}(x) \triangleq \frac{\mathrm{d}}{\mathrm{d}x}F_{\gamma_{\text{IQI}}}(x)$, the SINR PDF, in the presence of IQI, is given by

$$f_{\gamma_{\text{IQI}}}(x) = \frac{\alpha A e^{-\frac{A}{\overline{\gamma}\left(\frac{\alpha}{x}-\beta\right)}}}{\overline{\gamma}\left(\alpha-x\beta\right)^2} \tag{11}$$

which is valid for $0 \le x \le \frac{\alpha}{\beta}$.

**Lemma 1.** *For single-carrier systems impaired by IQI, the MGF of the instantaneous fading SINR is given by*

$$\mathcal{M}_{\gamma_{\text{IQI}}}(s) = e^{\frac{\alpha}{\beta}s+\frac{A}{\beta\overline{\gamma}}}\Gamma\left(1,\frac{A}{\overline{\gamma}\beta};\frac{s\alpha A}{\beta^2\overline{\gamma}}\right) \tag{12}$$

*where* $\Gamma(\alpha,x;b) = \int_x^\infty t^{\alpha-1}e^{-t-\frac{b}{t}}\mathrm{d}t$ *is the extended upper incomplete Gamma function [16].*

*Proof.* By recalling that [15]

$$\mathcal{M}_{\gamma_{\text{IQI}}}(s) = \int_0^\infty e^{sx}f_{\gamma_{\text{IQI}}}(x)\,\mathrm{d}x \tag{13}$$

and substituting (11) into (13), we obtain

$$\mathcal{M}_{\gamma_{\text{IQI}}}(s) = \int_0^{\frac{\alpha}{\beta}} e^{sx}\frac{\alpha A e^{-\frac{A}{\overline{\gamma}\left(\frac{\alpha}{x}-\beta\right)}}}{\overline{\gamma}\left(\alpha-x\beta\right)^2}\mathrm{d}x. \tag{14}$$

By also considering the change of variable $y = \alpha-\gamma\beta$ and after some mathematical manipulations yields

$$\mathcal{M}_{\gamma_{\text{IQI}}}(s) = \frac{\alpha A}{\overline{\gamma}\beta}e^{\frac{\alpha}{\beta}s+\frac{A}{\beta\overline{\gamma}}}\int_0^\alpha e^{-\frac{sy}{\beta}-\frac{\alpha A}{\beta\overline{\gamma}y}}\mathrm{d}y. \tag{15}$$

Based on this and by taking $z = \alpha A/(\beta\overline{\gamma}y)$, equation (12) is deduced, which completes the proof. □

## IV. Symbol Error Rate Analysis

This section capitalizes on the derived MGF representation and evaluates the SER performance of different coherent and non-coherent *M*-ary modulation schemes in the presence of IQI and multipath fading.

### A. Coherent $M$-PSK Symbol Error Rate Analysis

For coherently detected *M*-PSK, the SER under AWGN is given by [15, eq. (8.22)]

$$P_{s,\text{PSK}} = \frac{1}{\pi}\int_0^{\frac{(M-1)\pi}{M}}\exp\left(-\gamma\frac{g_{\text{PSK}}}{\sin^2(\theta)}\right)\mathrm{d}\theta \tag{16}$$

where $\gamma$ is the instantaneous SNR and $g_{\text{PSK}} = \sin^2(\pi/M)$. Under fading conditions, the average SER is obtained by averaging (16) over the corresponding SINR PDF, namely

$$P_{s,\text{PSK}} = \frac{1}{\pi}\int_0^\infty\int_0^{\frac{(M-1)\pi}{M}}\exp\left(-x\frac{g_{\text{PSK}}}{\sin^2(\theta)}\right)f_\gamma(x)\,\mathrm{d}\theta\mathrm{d}x \tag{17}$$

which is equivalent to

$$P_{s,\text{PSK}} = \frac{1}{\pi}\int_0^{\frac{(M-1)\pi}{M}}\mathcal{M}_{\gamma_{\text{IQI}}}\left(-\frac{g_{\text{PSK}}}{\sin^2(\theta)}\right)\mathrm{d}\theta. \tag{18}$$

Therefore, by assuming PSK modulation, the average SER in the presence of IQI is obtained by substituting the derived MGF expressions into (18), yielding

$$\begin{aligned}P_{s,\text{PSK}} = \frac{1}{\pi}\int_0^{\frac{(M-1)\pi}{M}} & e^{-\frac{g_{\text{PSK}}\alpha}{\sin^2(\theta)\beta}+\frac{A}{\beta\overline{\gamma}}} \\ & \times\Gamma\left(1,\frac{A}{\overline{\gamma}\beta},-\frac{g_{\text{PSK}}\alpha A}{\sin^2(\theta)\beta^2\overline{\gamma}},1\right)\mathrm{d}\theta.\end{aligned} \tag{19}$$

### B. Differential $M$-PSK Symbol Error Rate Analysis

Considering differential detection of *M*-PSK under AWGN, the exact SER is given by [15, eq. (8.90)], namely

$$P_{s,\text{DPSK}} = \frac{1}{\pi}\int_0^{\frac{(M-1)\pi}{M}}\exp\left(-\gamma\frac{g_{\text{PSK}}}{1+\rho\cos(\theta)}\right)\mathrm{d}\theta \tag{20}$$

where $\rho = \sqrt{1-g_{\text{PSK}}}$. Based on this and assuming Rayleigh fading conditions, and TX and/or RX IQI, the above expression can be expressed as

$$P_{s,\text{DPSK}} = \frac{1}{\pi}\int_0^{\frac{(M-1)\pi}{M}}\mathcal{M}_{\gamma_{\text{IQI}}}\left(-\frac{g_{\text{PSK}}}{1+\rho\cos(\theta)}\right)\mathrm{d}\theta. \tag{21}$$

The average symbol error rate for $M$-DPSK over Rayleigh fading channels in the presence of IQI is obtained by substituting the derived MGF expressions in (21), yielding

$$P_{s,\mathrm{DPSK}} = \frac{1}{\pi}\int_0^{\frac{(M-1)\pi}{M}} e^{-\frac{\alpha}{\beta}\frac{g_{\mathrm{PSK}}}{1+\rho\cos(\theta)}+\frac{A}{\beta\overline{\gamma}}} \times \Gamma\left(1, \frac{A}{\overline{\gamma}\beta}; \frac{-g_{\mathrm{PSK}}\alpha A}{(1+\rho\cos(\theta))\,\beta^2\overline{\gamma}}\right) \mathrm{d}\theta. \tag{22}$$

### C. Noncoherent $M$-FSK Symbol Error Rate Analysis

Assuming noncoherent detection of orthogonal signals, corresponding to a minimum frequency spacing $\Delta f = 1/T_s$ [15], the SER of $M$-FSK under AWGN is given by [15, eq. (8.66)], namely

$$P_{s,\mathrm{FSK}} = \sum_{k=1}^{M-1}(-1)^{k+1}\binom{M-1}{k}\frac{\exp\left(-\gamma\frac{k}{k+1}\right)}{k+1} \tag{23}$$

which under fading conditions is expressed as follows

$$P_{s,\mathrm{FSK}} = \sum_{k=1}^{M-1}\frac{(-1)^{k+1}}{k+1}\binom{M-1}{k}\mathcal{M}_{\gamma_{\mathrm{IQI}}}\left(-\frac{k}{k+1}\right). \tag{24}$$

Therefore, substituting the derived MGF expressions in (24) yields the average SER in the presence of IQI as

$$P_{s,\mathrm{FSK}} = \sum_{k=1}^{M-1}\frac{(-1)^{k+1}}{k+1}\binom{M-1}{k}e^{-\frac{\alpha}{\beta}\frac{k}{k+1}+\frac{A}{\beta\overline{\gamma}}} \times \Gamma\left(1, \frac{A}{\overline{\gamma}\beta}; \frac{-k\alpha A}{(k+1)\,\beta^2\overline{\gamma}}\right). \tag{25}$$

To the best of the authors' knowledge, the derived analytic expressions have not been previously reported in the open technical literature. It is also worth noting that the SER of $M$-QAM modulation can also be obtained from the derived MGFs. Furthermore, the analysis can be straightforwardly extended to the case of $L$-branch maximal ratio combining (MRC) diversity system [15], [17].

## V. Numerical and Simulation Results

In this section, we quantify the effects of IQI on the performance of single-carrier based $M$-PSK, $M$-DPSK and $M$-FSK systems over Rayleigh fading channels in terms of the corresponding average SER. For a fair comparison, we assume that the transmit power level is always fixed. This implies that the transmitted signal is normalized by $|\mu_t|^2+|\nu_t|^2$ for TX IQI, by $|\mu_r|^2+|\nu_r|^2$ for RX IQI and by $\left(|\mu_t|^2+|\nu_t|^2\right)\left(|\mu_r|^2+|\nu_r|^2\right)$ for joint TX/RX IQI.

To this end, Figs. 1−4 illustrate the SER for $M$-PSK, $M$-DPSK and $M$-FSK constellations, where all possible combinations of ideal/impaired TX/RX are presented. It is noted that the numerical results are shown with continuous lines, whereas markers are used to illustrate the respective computer simulation results. It is noticed that the derived expressions characterize accurately the simulated SER performance for all considered modulation schemes in the presence of IQI. This demonstrates that the approximations adopted in (7) does not significantly affect the accuracy of the SER analysis.

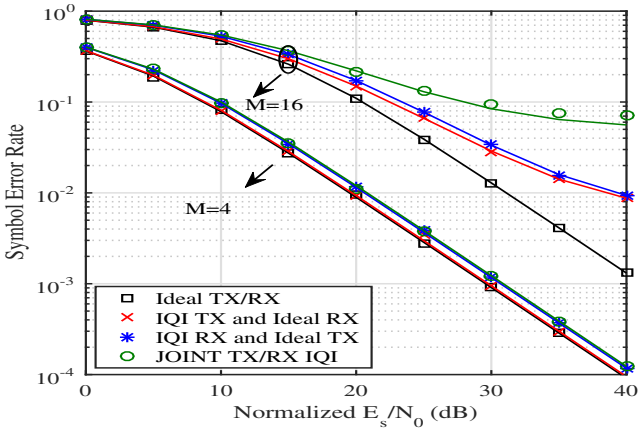


Fig. 1: Average SER as a function of the normalized $E_s/N_0$ for $M$-PSK when $\mathrm{IRR}_t = \mathrm{IRR}_r = 20\mathrm{dB}$ and $\phi = 3°$.

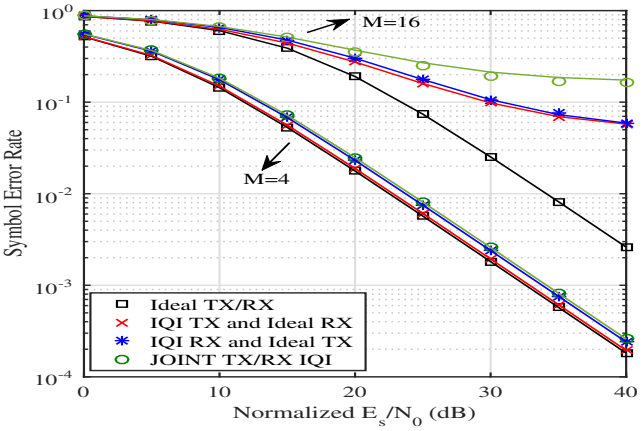


Fig. 2: Average SER as a function of the normalized $E_s/N_0$ for $M$-DPSK when $\mathrm{IRR}_t = \mathrm{IRR}_r = 20\mathrm{dB}$ and $\phi = 3°$.

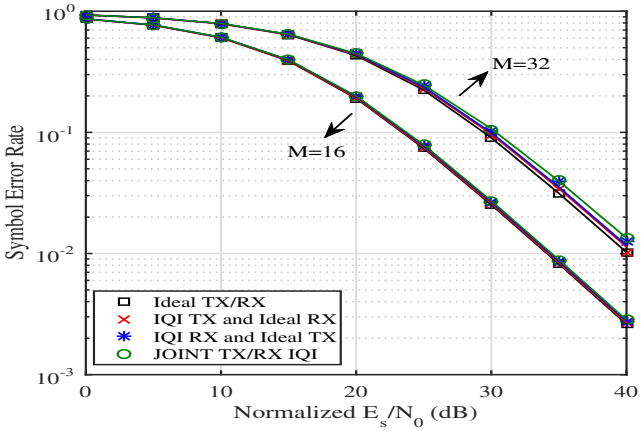


Fig. 3: Average SER as a function of the normalized $E_s/N_0$ for $M$-DPSK when $\mathrm{IRR}_t = \mathrm{IRR}_r = 35\mathrm{dB}$ and $\phi = 1°$.

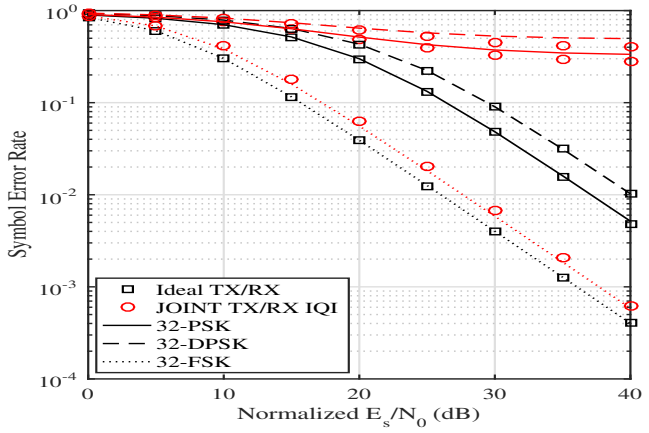


Fig. 4: Average SER as a function of the normalized $E_s/N_0$ for 32-PSK, 32-DPSK and 32-FSK when $\mathrm{IRR}_t = \mathrm{IRR}_r = 20\mathrm{dB}$ and $\phi = 3°$.

Specifically, it is first observed that RX IQI has, overall, more detrimental impact on the system performance than TX IQI. This result is expected since RX IQI affects both the signal and the noise while TX IQI impairs the information signal only. However, in some cases, e.g., in higher order modulations of PSK and DPSK, TX IQI causes performance degradation that is quite comparable to the RX IQI. It is also noticed that IQI exhibits different levels of degradation on the performance of the different modulation schemes considered. For example, it is shown in Fig. 4 that joint TX/RX IQI only slightly affects the performance of 32-FSK. It is further noted that the effects of IQI on FSK are rather limited irrespective of the modulation order. On the other hand, it is shown that IQI causes an error floor for the other two candidate modulation schemes. This can be explained by the fact that the tone spacing in FSK is constant regardless of the modulation order. Hence, unlike PSK and DPSK, the IQI effects on FSK do not depend on the modulation order. However, the cost of increasing $M$ for FSK is increase of the transmission bandwidth. This is not the case for the other two modulation schemes where the angle separation depends on the modulation order. For instance, the effects of IQI can be considered acceptable i.e., no error floor is observed for the considered SNR range, only for $M = 4$ for PSK and DPSK based systems. In fact, when $M = 16$, an error floor is observed at around $35\mathrm{dB}$ when PSK modulation suffers from joint TX/RX IQI, while for DPSK this error floor appears at around $30\mathrm{dB}$ for all the considered impairment scenarios. It is also worth noting that for the joint TX/RX IQI case, this error floor is around $6 \times 10^{-2}$ for PSK versus $2 \times 10^{-1}$ for DPSK. Hence for a fixed $M$, the error floor is higher for DPSK than PSK.

## VI. Conclusion

We developed a general framework for the SER performance analysis of different $M$-ary coherent and non-coherent modulation schemes over Rayleigh fading channels in the presence of IQI at the RF front end. The realistic cases of TX IQI only, RX IQI only and joint TX/RX IQI were considered and the corresponding average SER expressions of the underlying schemes were derived, providing useful insights into the overall system behavior. The derived analytic results were corroborated with respective results from computer simulations. It was shown that the performance degradation caused by IQI depends on the considered modulation scheme with $M$-DPSK being the most sensitive modulation scheme to IQI. Moreover, for coherent and noncoherent phase modulations, increasing the modulation order increases the impact of IQI on the system, while for the case of frequency modulation the performance degradation observed is constant regardless of the modulation order. To this effect, it was shown that frequency modulation is the most robust scheme to IQI effects.

## References


[1] S. Mirabbasi and K. Martin, "Classical and modern receiver architectures," *IEEE Commun. Mag.*, vol. 38, no. 11, pp. 132–139, Nov 2000.

[2] S. Bernard, "Digital communications fundamentals and applications," *Prentice Hall, USA*, 2001.

[3] A. Gokceoglu, Y. Zhou, M. Valkama, and P. C. Sofotasios, "Multi-channel energy detection under phase noise: analysis and mitigation," *ACM/Springer Journal on Mobile Networks and Applications (MONET)*, vol. 19, no. 4, pp. 473−486, Aug. 2014.

[4] J. Abouei, K. N. Plataniotis, and S. Pasupathy, "Green modulations in energy-constrained wireless sensor networks," *IET Commun.*, vol. 5, no. 2, pp. 240–251, 2011.

[5] A. Manolakos, M. Chowdhury, and A. J. Goldsmith, "Constellation design in noncoherent massive SIMO systems," in *IEEE Globecom '14*, Dec. 2014, pp. 3690–3695.

[6] B. Natarajan, C. R. Nassar, and S. Shattil, "CI/FSK: bandwidth-efficient multicarrier FSK for high performance, high throughput, and enhanced applicability," *IEEE Trans. Commun.*, vol. 52, no. 3, pp. 362–367, Mar. 2004.

[7] F. F. Digham, M. S. Alouini, and S. Arora, "Variable-rate variable-power non-coherent M-FSK scheme for power limited systems," *IEEE Trans. Wireless Commun.*, vol. 5, no. 6, pp. 1306–1312, Jun. 2006.

[8] C. Zhu, J. Cheng, and N. Al-Dhahir, "Error rate analysis of subcarrier QPSK with receiver I/Q imbalances over Gamma-Gamma fading channels," in *ICNC'17*, Jan. 2017, pp. 88–94.

[9] B. Selim, P. C. Sofotasios, S. Muhaidat, G. K. Karagiannidis, and B. Sharif, "Performance of differential modulation under RF impairments," in *IEEE ICC '17*, May 2017, pp. 1–6.

[10] K. Kiasaleh and T. He, "On the performance of DQPSK communication systems impaired by timing error, mixer imbalance, and frequency nonselective slow Rayleigh fading," *IEEE Trans. Veh. Technol.*, vol. 46, no. 3, pp. 642–652, Aug 1997.

[11] L. Chen, A. Helmy, G. R. Yue, S. Li, and N. Al-Dhahir, "Performance analysis and compensation of joint TX/RX I/Q imbalance in differential STBC-OFDM," *IEEE Trans. Veh. Technol.*, vol. 66, no. 7, pp. 6184−6200, Jul. 2017.

[12] L. Chen, A. G. Helmy, G. Yue, S. Li, and N. Al-Dhahir, "Performance and compensation of I/Q imbalance in differential STBC-OFDM," in *IEEE Globecom'16*, Dec 2016, pp. 1–7.

[13] T. Schenk, *RF Imperfections in High-Rate Wireless Systems*. The Netherlands: Springer, 2008.

[14] A. A. A. Boulogeorgos, P. C. Sofotasios, B. Selim, S. Muhaidat, G. K. Karagiannidis, and M. Valkama, "Effects of RF impairments in communications over cascaded fading channels," *IEEE Trans. Veh. Technol.*, vol. 65, no. 11, pp. 8878–8894, Nov 2016.

[15] M. K. Simon and M.-S. Alouini, *Digital communication over fading channels*. John Wiley & Sons, 2005.

[16] M. A. Chaudhry and S. M. Zubair, *On a class of incomplete gamma functions with applications*. CRC press, 2001.

[17] B. Selim, O. Alhussein, S. Muhaidat, G. K. Karagiannidis, and J. Liang, "Modeling and analysis of wireless channels via the mixture of gaussian distribution," *IEEE Trans. Veh. Technol.*, vol. 65, no. 10, pp. 8309–8321, Oct 2016.